Hydro-Electric Power Optimisation Service

31811900

March 2024

In July of 2018, Typhoon Prapipoon resulted in heavy rains across south-western Japan, which resulted in extreme rainfall accumulations. This resulted in major flooding in Shikoku and west Honshu in south Japan which caused 225 deaths and property damage of approximately US$10 billion.

One way of reducing the impacts of such disasters is through the management of dams associated with hydroelectric power stations. One potential way is to use forecasts to plan for the management of dam levels, so that water levels can be reduced when extreme rainfall events are forecasted to ensure that dam overtopping, which results in flooding downstream, does not occur.

In the project, I used and adapted version of the Hirsch et al. (2014) dam operation model which maximises total power generation over the time period inputted, while maintaining a head level within the minimum and maximum values at the damn, as well as well as maintaining a flow rate within the minimum and maximum set. I investigated the use of this model in the context of the Tokuyama dam in southwestern Honshu, the largest dam in Japan. It is located at $35.667°N, 136.502°E$, and has a reservoir area of $13km^2$, and a hydrological catchment area of $254km^2$. The height of the dam, H_{dam} is $161m$, the maximum power generation, G_{max} is 153MW and the energy conversion efficiency, σ is 0.9.

The parameters used to constrain the model are the minimum and maximum heads of water at the dam, H_{min}, H_{max}, the minimum and maximum flow rates, W_{min} and W_{max} , the reservoir emptying timescale, τ, and the maximum power generation rate G_{max}. The dam also has a maximum relief flow, R_{max}, that is not constrained by the model. The default values are listed in Table 1.

Parameter	Value
H_{min}	$0.5 \times H_{dam}$
H_{max}	$0.2 \times H_{dam}$
τ	180 days
W_{max}	$0.5 \times A \times H_{dam}/\tau$
W_{min}	$0.1 \times W_{max}$
R_{max}	$0.1 \times W_{max}$

Table 1: Default parameters for the Tokuyama dam

In this project, I investigated the models behaviour and investigated the possibility of using S2S forecasts with the dam optimisation model to assist with dam management.

1 Model Investigation

1.1 Time Range

An initial investigation on how the time period of the data inputted into the model changes the results of the model. For this, ERA5 runoff data, in units of m, of the grid point closest to the dam location $(35.7N, 136.5E)$ was used. Using a map, the dam and its catchment area was within the grid selected. I thus did not include data from any other grid points.

Data spanning a range of time periods beginning from 1 June in both 2017 and 2018 were inputted to the model. Figure 1(a), (b) and (c) show the optimised flow rate, relief flow and water head level produced by the model for time ranges of 1, 2, 3, 4 and 6 months.

The water head levels in the dam for a time period of 1 month in both 2017 and 2018 show that the model maximises the power generated by letting as much water flow out as possible. While this maximises power generation in the short term, it is not a sensible solution in the long term, as it reduces the amount of power that can be generated after this due to the lowered water head levels (Figure 1(c)). From Figure 1(b) that there is a large relief flow, indicating that the potential energy of large amounts of water are not used for generating hydropower, as they bypass the generator. This is thus not a sensible solution, and suggests that a time period of one month is too short.

For a time range of two and three months, the model returns negative flow rates, which are unphysical, thus suggesting that this time range does not give sensible results.

The solutions for time ranges of four and six months are similar, and do not have negative flow, suggesting that four months is the minimum time range needed for the model to produce a stable, plausible solution.

The water head at the dam does not fall within 15m of H_{min} and H_{max}, suggesting that the model is very conservative about the optimised water head levels, and follows the $H_{min} < H < H_{max}$ constraint well. This might result in the model not producing a solution that truly maximises power generation, as there is relief flow even though there is still space available in the dam to store water. This water could have been stored to release at a late date, when the flow rate was lower, resulting in a larger amount of power generated in total.

Across all the time ranges, relief flow is observed when the optimised flow rate reaches W_{max}, showing that the model works well in applying the $W < W_{max}$ constraint to the solution. The only condition the model fails to constrain is $W > W_{min}$ (Figure 1(a)), with all solutions having $W < W_{min}$ at some point, and some solutions even having unphysical, negative flow. Since all solutions have $W > W_{min}$, as long as flow is positive, we consider it a plausible solution as long as all values of flow are positive.

The model does not constrain the relief flow, which is $0.2 \times W_{max}$ in the dam we are studying. From Figure 1(b), the relief flow exceeds W_{max}, even reaching $2 \times W_{max}$, during periods of high runoff. Instead of keeping the water in the dam and increasing the dam head level, the model opts to get rid of the excess water using relief flow, which is unrealistic. This can also be seen in Figure 1(b), where the relief flows tend to be large, over a short period of time. The model is likely too conservative in the water head levels, thus resulting in large flowrates and unrealistic relief flows during periods with large amounts of runoff.

From Figure 1(c), the water head levels at the dam are different for different runs, even though the starting date is the same. This is because the model also solves for the initial dam value. This does not make sense in a forecasting context, as the dam will have a pre-existing water head level, and it might not be possible to change the water head level to the model solution, especially if the solution is larger than the existing water head level.

1.2 Dependence on $H_{max}.H_{min}$ and W_{max}

To investigate the model dependence on the inputs defining the constraints, H_{max}, H_{min} and W_{max} were varied and plotted the optimised solutions for flow rate and water head for runoff data from 1 June to 30 September 2017.

To investigate the models dependence on H_{max}, the model was run for 3 values of H_{max}, 80%, 100% and 120% of the default H_{max}, corresponding to $H_{max} = 64.4m, 80.5m$ and $96.6m$ respectively. Figure 2(a) shows that there is no consistent impact on the solution for flow rate, as on some dates, larger H_{max} results in a larger flow rate, while on other dates, larger H_{max} results in a smaller flow rate. Overall, the solutions for flow rate are very similar. The differences in the solutions are small, and could be a result of coming from different runs of the model, since the model does not generate generate the same solution from the same data each time it is run. From Figure 2(b), H_{max} appears to have a large impact on the model solution for the initial water head level, with larger H_{max} resulting in a larger initial water head level. The trend in water head over time is very similar, a result of the similar trends in flow rates. This leads to final water head levels for larger H_{max}.

The model's dependence on H_{min} was investigated in the same was as H_{max}, with $H_{min} = 12.9m, 16.1m$ and $19.3m$ being used. A similar trend to H_{max} was found, with flow rate not varying much with H_{min}, and the initial and final water head levels being smaller for smaller H_{min} (Figure 3). The difference between water heads for different H_{min} are smaller than for H_{max}, due to the differences in the different values being smaller, since $H_{min} < H_{max}$.

The model's dependence on W_{max} was investigated in the same way as H_{min} and H_{max}, with $W_{max} = 53.8m^3s^{-1}, 67.3m^3s^{-1}$ and $80.7m^3s^{-1}$ being used. W_{min} is also varied, since $W_{min} = 0.1W_{max}$. Contrary to H_{min} and H_{max}, Figure 4(a) shows that there is a variation in the flow rate solutions with W_{max}, where larger W_{max} generally has larger flow rate solutions, especially early in the solution. The solutions become more similar with time, and are very similar from approximately 22 August onward, and have identical solutions in the last 20 days of the solution. From Figure 4(b), a larger W_{max} results in a larger initial water head level. Unlike for H_{min} and H_{max}, the differences in water head level reduces with time, appearing to converge in mid-August. This suggests that W_{max} has an impact on initial water head levels, but not on the long-time solution for the water head level are the same. W_{max} also has an impact on the amount of relief flow if W reaches W_{max}, since a lower W_{max} would result in more flow avoiding the turbines.

Overall, it appears that H_{min} and H_{max} do not have a great impact on the flow rate solution, but have an impact on the overall solution for water head level, while W_{max} has an impact on the flow rate solution and the initial water head level, but the solution for flow rate tends to converge over time for different W_{max} if large flow rates close to W_{max} are not observed. The solution for water head level at longer times (~ 2.5 months) converges, suggesting that W_{max} does not impact long term water head level solutions.

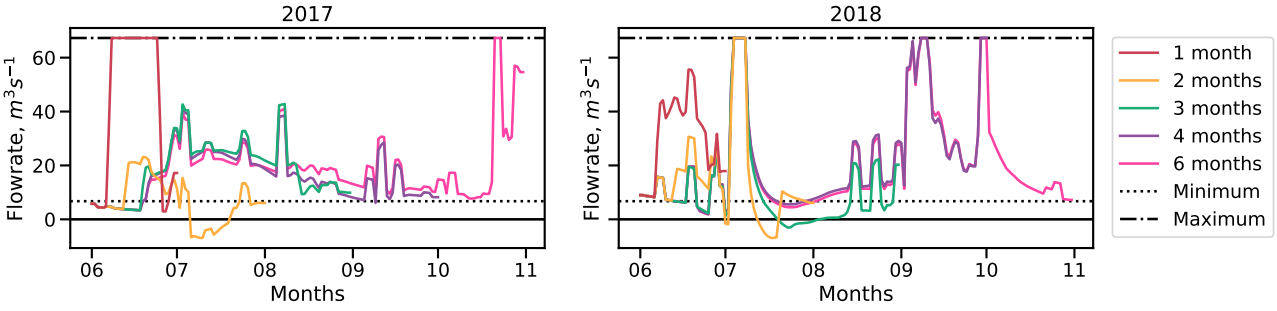

(a) Flowrate

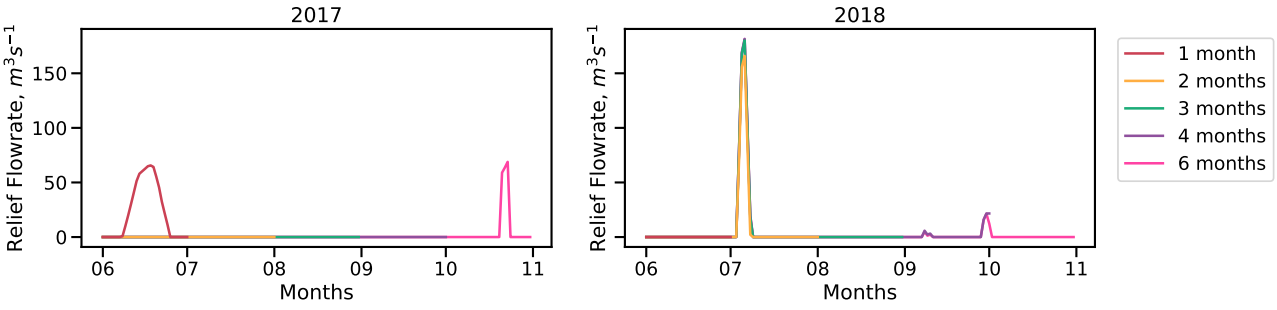

(b) Relief Flow

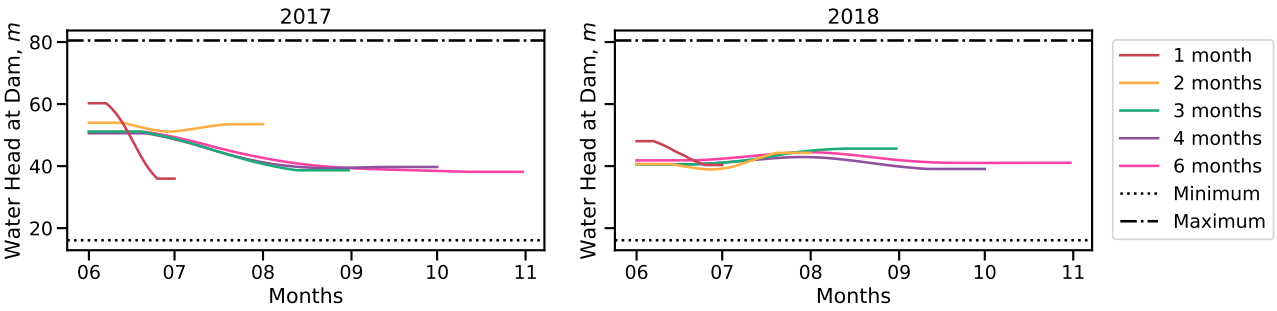

(c) Waterhead at Dam

Figure 1: Dam optimisation solutions for (a) flow rate, (b) relief flow, and (c) water head at the dam for a range of time periods beginning on 1 June for 2017 (left) and 2018 (right).

2 Seasonal to Sub-Seasonal (S2S) Forecasts

The model could be used to plan for dam management through the usage of Seasonal to Sub-seasonal (S2S) forecasts. This could help to plan for forecasted dry periods, or periods of intense rainfall that could lead to high levels of runoff. This would allow the dam management to plan water head levels in the dam before the event to prevent the dam drying out or overtopping.

2.1 ERA5 Upscaling

The S2S forecasts have a grid size of $1.5° \times 1.5°$, while the ERA5 data has a grid size of $0.1° \times 0.1°$. To effectively compare the two datasets, the ERA5 data has to be upscaled to a $1.5° \times 1.5°$ grid. This is done by taking an average of the runoff values in a square of 17×17 ERA5 grids centred on the grid used in the ERA5 data above. Since the $1.5° \times 1.5°$ grid does not completely cover this square, only the values on the edges were weighted by 0.5 and those on the corner were weighted by 0.25 to accurately represent the fraction of those grids overlapping with the S2S grid.

Since the upscale runoff is an average of runoff from a larger area around the dam, the runoff is no longer as representative of the runoff into the dam. To investigate this, I plotted the ERA5 runoffs against the upscaled ERA5 runoffs for 1 June 2017 to 31 May 2018 5(a). Since both ERA5 and ERA5 upscaled runoffs have the same set of dates, a paired calibration was performed, using a linear fit such that

$$RO_{ERA5} = RO_{UpscaledCalibrated} = m \times RO_{Upscaled} + c, \tag{1}$$

where RO is the runoff. Using least-squares regression, m was found to be 1.10 ± 0.01 while c was found to be

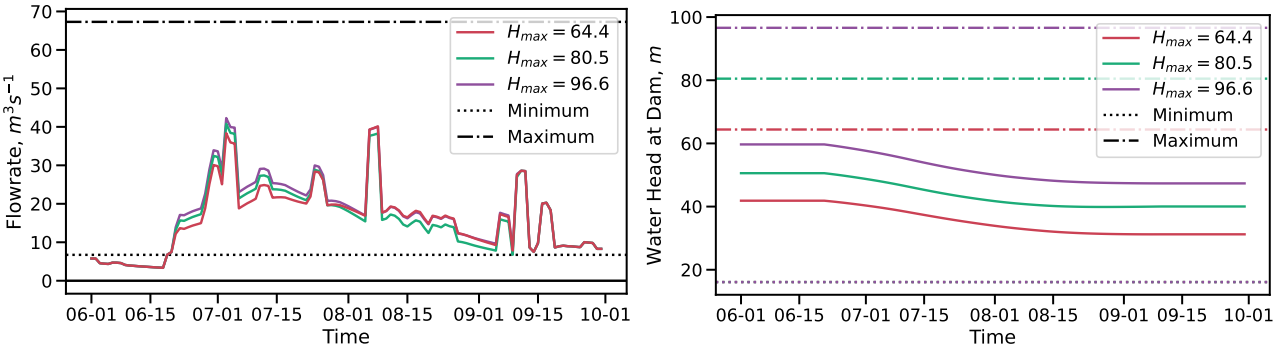

(a) Flowrate (b) Water Head

Figure 2: Model solution for (a) flow rate and (b) water head at the dam for a range of H_{max} values. The maximum water head levels are plotted for each H_{max} in the corresponding color in (b).

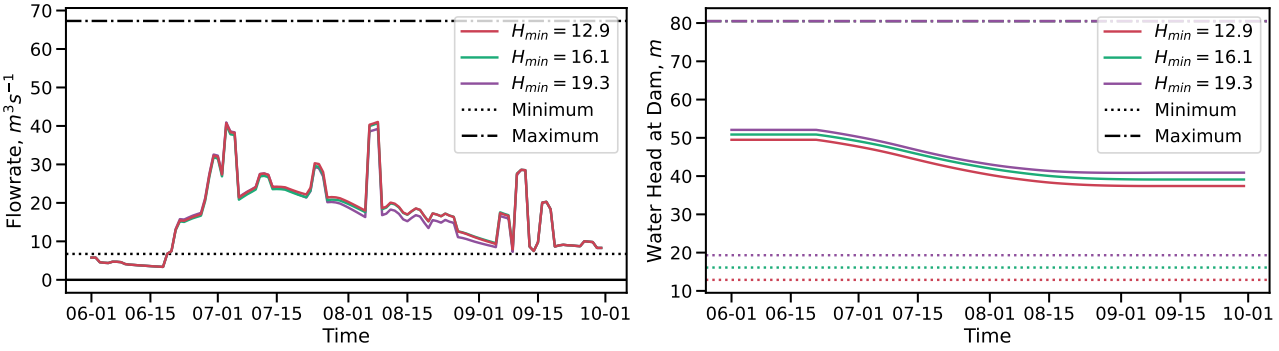

(a) Flowrate (b) Water Head

Figure 3: Model solution for (a) flow rate and (b) water head at the dam for a range of H_{min} values. The minimum water head levels are plotted for each H_{min} in the corresponding color in (b).

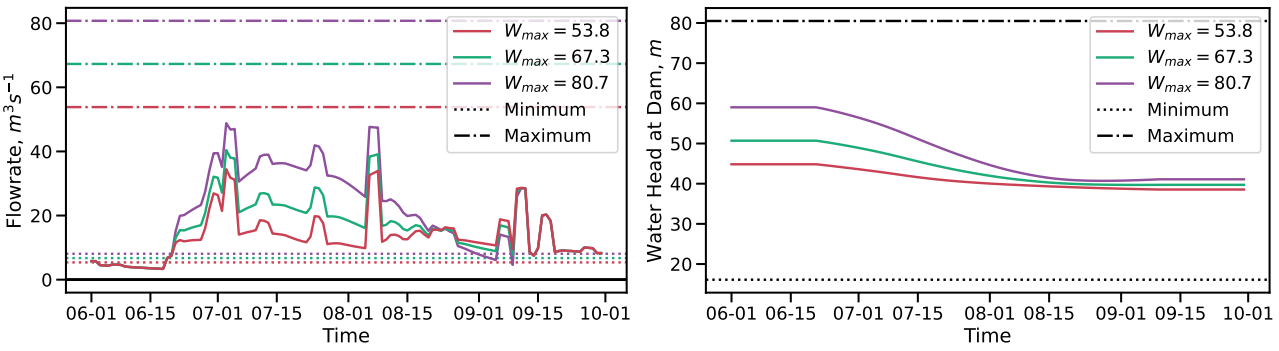

(a) Flowrate (b) Water Head

Figure 4: Model solution for (a) flow rate and (b) water head at the dam for a range of H_{max} values. The maximum and minimum flow rates are plotted for each W_{max} in the corresponding color in (a).

$(4 \pm 1) \times 10^{-4} m$ The calibrated upscaled ERA5 runoff is plotted against the original ERA5 data in Figure 5(b), and the runoff values appear to fall closer to the 1:1 line in general, suggesting that the calibration brought the upscaled data closer to the original data.

This calibration is unlikely to fully correct the differences between the two data, as the ERA5 upscaled runoff is averaged over surrounding areas, with a total grid length of about $160km$. The distribution of runoff across the surrounding areas is likely to vary across time, as some areas will get more runoff due to more rain over specific regions, especially considering that the grid can be larger than larger convective systems, such as some mesoscale convective systems, which begin at a span of about 100km (Society, 2012).

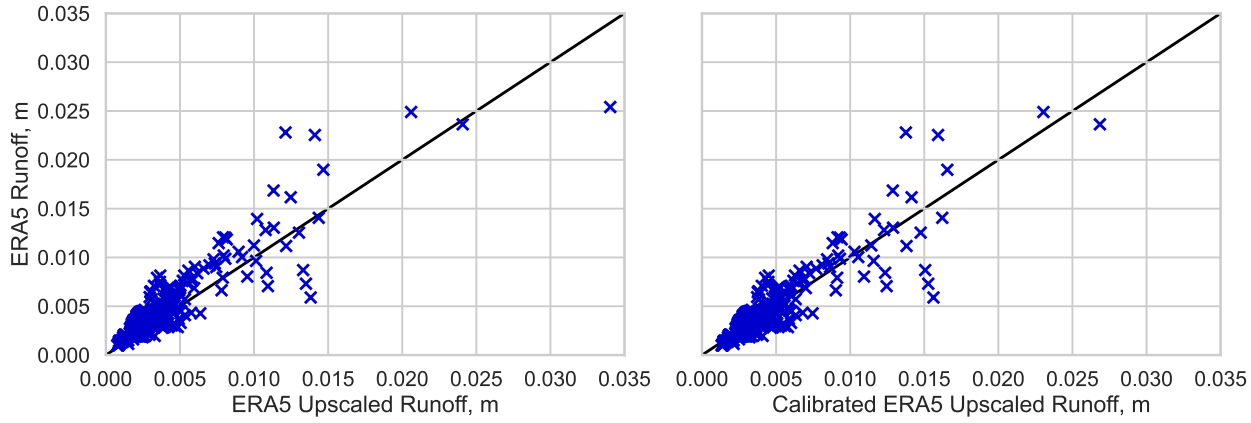

(a) (b)

Figure 5: ERA5 Runoff against ERA5 Upscaled Runoff for dates between 2017-06-01 and 2018-05-31. (a) shows the original data, and (b) shows the data after paired calibration. The black line in both plots is the 1:1 line.

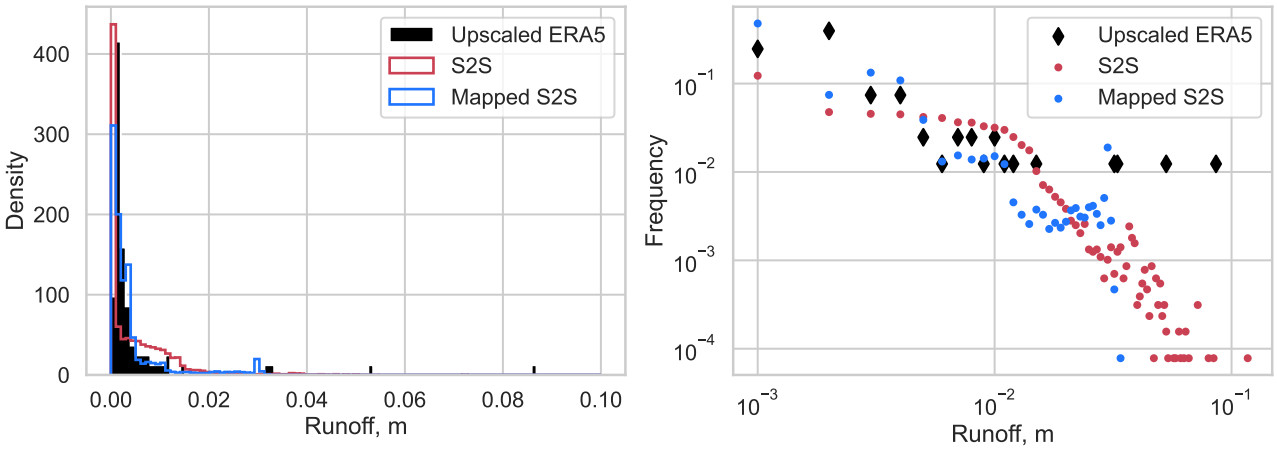

(a) (b)

Figure 6: (a) Histogram and (b) plot of log-binned runoff values from Upscaled ERA5 data, Meteo France S2S data, and quantile-quantile mapped Meteo France S2S data. The density in the plot in (a) is more than 1 as the bin heights are scaled such that the areas of the bars sum to 1, and the bin-widths are 0.001m.

2.2 S2S Statistics

The S2S forecasts from Meteo France for June-August of 2017 and 2019 were used to investigate the statistics of the S2S runoff data. The runoff is recorded as the accumulation of runoff from the start of the forecasts, and was thus converted into runoff per day by subtracting the value from the previous day. The runoff is also given in units of kgm^-2, and was converted to units of m by dividing by water density, $1000kgm^-3$.

To visualise the distribution of the S2S data compared to the ERA5 data, histograms of runoff values from S2S forecasts were plotted. There were 9 forecasts in summer, and 8 in 2019, each with 50 ensemble members. These forecasts spanned 2017-06-02 to 2017-08-28 and 2019-06-07 to 2019-08-26, but the 2019 forecasts were limited to before 2019-08-01, as ERA5 data was not available for dates beyond this. A histogram of the upscaled ERA5 runoff for these time periods was also plotted. Both 2017 and 2019 were used as the forecast data was only available in the summer. This meant that the ERA5 runoff dataset would be sparse, with less than 90 data points, if only one year was used. Data from 2018 was not used, as it would bias the calibration when investigating 2018 data.

The forecasts are 32 days long, and are started a week after the previous forecast. This means that the forecasts are overlapping. The S2S runoff values used are therefore likely to be biased toward the middle of summer, where the number of forecasts overlapping is greatest, resulting in days in the middle of summer being more over represented in the dataset, while days in the beginning and end are under represented, as only one forecast is contributing to those dates.

From Figure 6(a), the distributions of the upscaled ERA5 and the S2S runoffs look similar, with a high density at low runoff values, and lower densities at higher values. Looking more closely at different sections,

the S2S forecasts appears to over represent runoff values under 0.002m and between 0.005m-0.020m, and under represent values between 0.002m-0.005m, and above 0.020m.

I hypothesized that since runoff originates from rainfall, runoff might follow a similar distribution to rainfall, which follows a fat-tail distribution, which presents as a straight line when log-binned data is plotted on a log-log scale (Christensen and Maloney, 2005). The logbin function by McGillivray (2019) was used to bin the data in bins of exponentially increasing widths. The function only works on integer values so the runoff values were multiplied by 1000, and rounded to the nearest integer before log-binning. The bin centre values were then divided by 1000 after the function was run.

Both the upscaled ERA5 runoff values and the S2S forecast values were log-binned and plotted. From Figure 6(b), the upscaled ERA5 appears approximately linear, then appears flat at higher runoff values. This flat region is due to the sparsity of the data. The data is sparse, and thus the flat area corresponds to the bins which only on runoff value fall within. The trend is likely to be more linear at higher runoffs if a larger dataset is used. The S2S values follow a different trend, with a shallower gradient than the gradient for the upscaled ERA5 data for runoffs below 10^{-2}, and a steeper gradient after. The over and under representation observed in Figure 6(a) is more clearly seen here.

Since the distributions in runoff values in the S2S forecasts differ greatly from the upscaled ERA5 data, the S2S forecast runoff values need to be calibrated to give accurate runoff values, allowing for accurate inflow into the dam to be calculation, and for useful solutions to be found by the model.

3 Calibration

Since the S2S forecast is not gaussian and has under and over representation in multiple ranges of run-off values, a simple scaling relation is unlikely to be effective in reconciling the distributions. I thus chose to do non-parametric quantile-quantile mapping, one of the best quantile mapping methods for rainfall, since runoff is highly correlated to rainfall Enayati et al. (2020). Quantiles in multiples of 5% (0%, 5%, 10%...) were calculated from the upscaled ERA5 data from 2017 and 2019 described in Section 2.2. Values for each quantile were then interpolated from this. Quantile values were not directly calculated from the data due to the sparsity of the data. The quantiles for each runoff value in the S2S data was then calculated, and mapped to the upscaled ERA5 quantile values.

The distributions of QQ-mapped the S2S runoff values are plotted in Figure 6(a) and (b). From Figure 6(a), the distribution is not exactly the same as the upscaled ERA5 data, but is much closer after calibration. The over representation of runoff values between 0.005 and 0.020m has been corrected, and the under representation for values larger than 0.020m has also improved. From Figure 6(b), the distribution for the QQ-mapped S2S runoff values is more linear, and has a gradient similar to the upscaled ERA5 values, expecially at lower values of run-off. It is difficult to evaluate the accuracy of the mapping at higher run-off values due to the sparsity of ERA5 data in this region.

The data was then further calibrated using the calibration calculated between the upscaled and the original ERA5 runoff data in Equation 1 order to most accurately represent the forecasted run-off values at the dam.

The QQ mapping performed is limited in that the upscaled ERA5 dataset used has less than 200 datapoints, and only spans two summers. This means that the calibration is not historically representative of runoff. The runoff distribution might vary slightly in different years, and given that there was an extreme rainfall event in the summer of 2018, the calibration might be over representing high runoff values compared to the true distribution of runoff over all time. Given that only data from between June and August was used, the is also unlikely to be representative of runoff throughout the whole year, due to the seasonality of rainfall and thus runoff. The data was limited to between June and August as the S2S forecast data only spanned June to August. If S2S forecast data was available for the whole year, the whole year of ERA5 data could be used, thus allowing for a more representative calibration. It is important that the two datasets used for the calibration span the same time period, as the calibration will not be accurate otherwise. QQ mapping might also be inaccurate for forecasted values beyond values seen in past forecasts, as there will not be observed data in percentiles beyond 100%. The values will be extrapolated from the observed values, and thus have the possibility of being unrealistic.

4 Optimisation

4.1 One S2S Forecast

The model was run for all 50 ensemble members of the forecast beginning 2018-29-27, approximately a week before the extreme rain event. Out of the 50 ensemble members, the model did not converge for 2 ensemble members, while 6 ensembles had solutions with negative flow. These unphysical solutions were discarded, leaving 42 ensemble members. The solution for the flow for each of these members was plotted and the ensemble mean solution as well as the 10^{th} and 90^{th} percentiles were calculated, as shown in Figure 7.

The solutions for most of the different ensemble members rapidly goes to the maximum flow, suggesting the solution has similar properties to the 1 month solution in Section 1.1, which maximises the flow to maximise the power generation over the short time period. This makes sense as the period of the forecast is 32 days, which is only 2 days more than the one month period in Section 1.1.This suggests that the period of one forecast is not long enough for reliable results.

The solutions are very similar for the first few days, which is due to the starting run-offs in the ensemble members being very similar to each other. They start to diverge after approximately 3 days, continuing to diverge with time until approximately 7 days before the end of the forecast, after which the variation decreases slightly, and then appears to be approximately constant. This decrease in variation could be a result of the rapid emptying of the dam to maximise power in the short period, which results in lower water head levels in the dam, and thus a lower flow rate at the end of the solution.

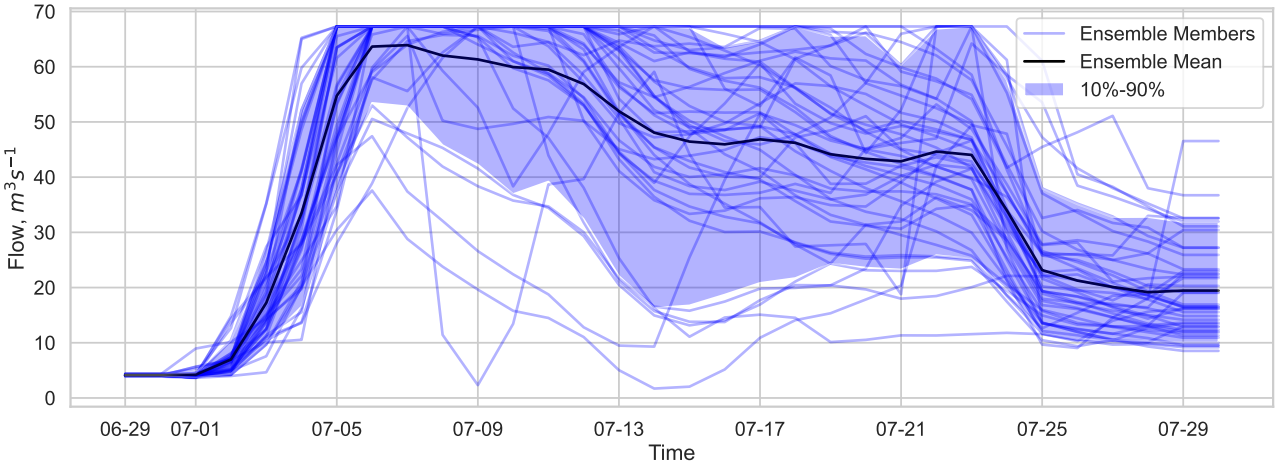

Figure 7: Flow solutions for 42 ensemble members and the mean ensemble solution for a single S2S forecast.

4.2 Extended Forecast

The time range of the runoff data inputted into the model was extended by using 3 months of upscaled ERA5 data from before the start date to extend the dataset. The input data set for the forecast beginning 2018-06-28 was thus 2018-03-28 to 2018-07-30. This is approximately 4 months, which should give a stable, plausible solution.

For comparison to the S2S solutions, the ERA5, upscaled ERA5 and calibrated upscaled ERA5 runoff values from the same time period were inputted into the model, and the solutions for flow were plotted (Figure 8, top). From the plot, the flow for the upscaled ERA5 runoff is generally smaller than the ERA5 runoff, and the solution for the calibrated upscaled ERA5 runoff is very similar to the upscaled ERA5 runoff, suggesting that the calibration was not very effective.

The model was run for all 50 ensemble members of the extended forecast. The model converged for all 50 ensemble members, but 2 ensembles had solutions with negative flow. These solutions were discarded, leaving 48 ensemble members, an improvement from the 42 members left in Section 4.1. As above, the flow solution for each members was plotted in addition to the ensemble mean and the 10^{th} and 90^{th} percentiles (8, middle).

The flows are homogeneous at the start of the solution, but begin to diverge approximately 20 days in. This divergence shows that the variation in runoff after the forecast start date affects the solution much before the forecast start date. Despite the divergence, the shape of the solution is very similar across the members. The variation in the solutions stays constant from 20 days until 5-6 days after the forecast starts, where it starts to diverge more. This is likely due to the runoffs across the ensemble members beginning to diverge several days after the forecast starts. From this point, the spread appears to be approximately constant to the end of the solution.

The ensemble mean solution of the extended S2S forecast appears very similar to the upscaled ERA5 solution up until the forecast starts. Beyond this, the mean solution is different from the upscaled ERA5 solution, but the $10^{th} - 90^{th}$ percentile range overlaps with the upscaled ERA5 solution, showing that the ensemble predicts the possibility of the upscaled ERA5 solution, up until approximately 15 days after the forecast starts. The 20 days after the forecast starts has an event with larger run-off, resulting in the flow increasing to the maximum flow in the upscaled ERA5 solution. This is replicated by many ensemble members, showing that the S2S data predicts this well. Beyond this, the flow decreases much more quickly in the upscaled ERA5 than in the S2S mean solution. This is also not captured in the $10^{th} - 90^{th}$ percentile range.

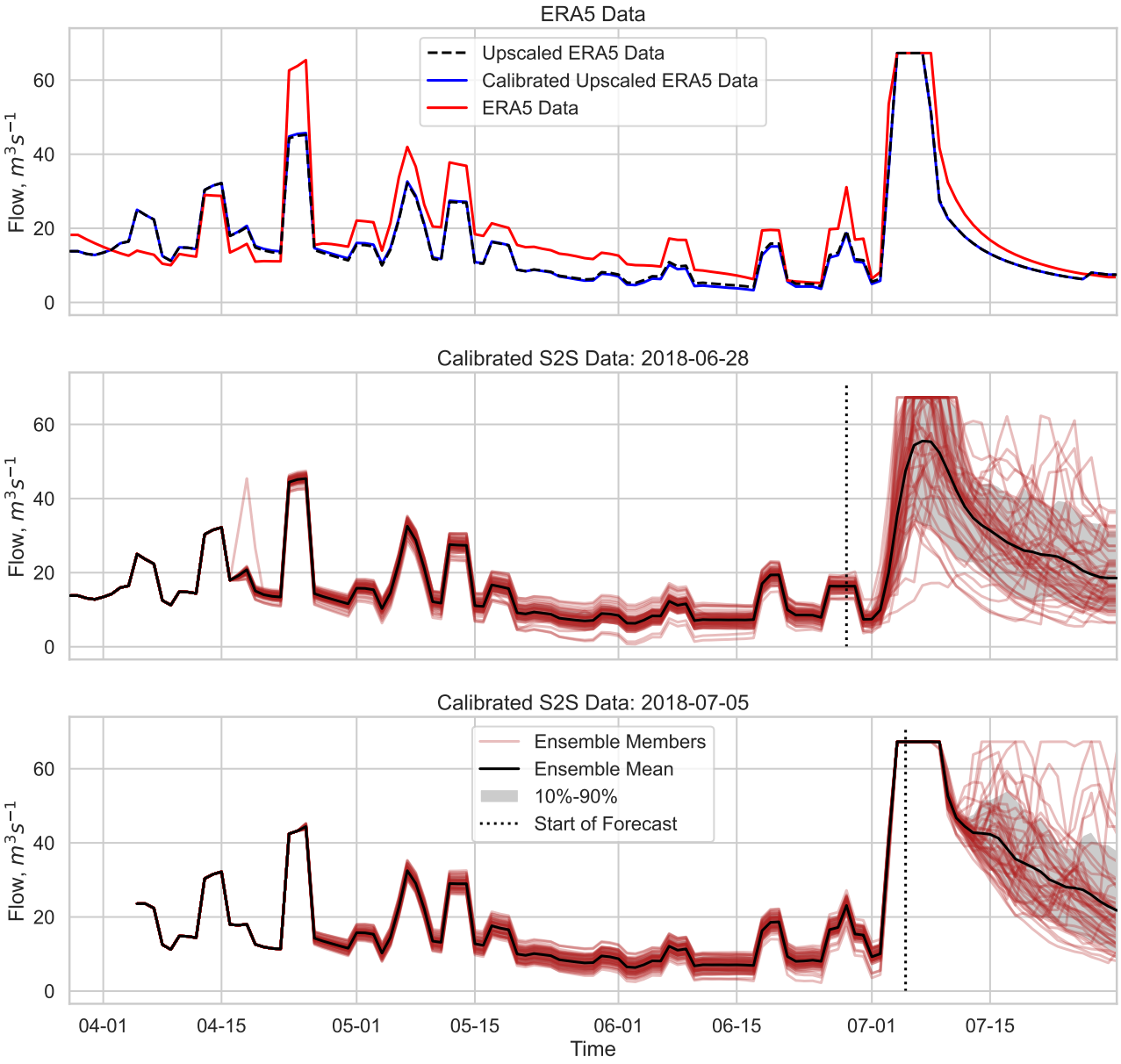

Figure 8: Model solutions for flow from 2018-03-28 to 2018-07-30. Top; Solutions for ERA5 data, upscaled ERA5 data and calibrated upscaled ERA5 data. Middle: Solutions for 48 ensemble members and ensemble mean solution of an extended S2S forecast, with the forecast beginning 2018-06-28. Bottom: Solutions for 47 ensemble members and ensemble mean solution of an extended S2S forecast, with the forecast beginning 2018-07-05.

One possible reason for this could be that this is during the latter half of the forecast, and the forecast has possibly lost skill. To test this, I repeated the extended forecast with the forecast beginning 2018-07-05, extended with upscaled ERA5 data beginning 2018-04-05 (Figure 8, bottom). Out of the 50 ensemble members, 47 returned physical solutions for flow. Despite the forecast being initialised a week later, the $10^{th} - 90^{th}$ percentile range of the solution does not capture the rapid drop seen in the solution for upscaled ERA5. This is thus unlikely to be related to when the forecast is started.

While the S2S extended forecast solution does not appear to replicate the lower flow rates seen after the flow reaches W_{max}, it does replicate the possibility of reaching W_{max} well. This is arguably more important than predicting the low flow, as not releasing enough water from the dam could result in flooding, but the slower decrease in flow rate after the event will likely only impact the amount of power generated by the dam, which is unlikely to have as large an impact as flooding.

The S2S extended forecast is good in producing similar results to the upscaled ERA5 data. This indicates that the QQ-mapping done above was effective in calibrating the S2S runoff data to observed runoff data. The S2S extended forecast is limited in that it is not able to produce results similar to the ERA5 data, which has a smaller grid size. However, this is not an issue with the S2S forecast skill, or the model, but with the calibration

of upscaled ERA5 runoff to ERA5 runoff.

Despite the difference in flow solutions between the extended forecast and the ERA5 data, both datasets produce similar trends with time, but with different magnitudes, where the magnitude of flow under ERA5 generally being larger than the solution from the forecast. Since the trend is similar, it could be used to inform the dam operators of how generally to control the flow. The flow from the forecast could also be scaled up to account for the difference in magnitude compared to ERA5.

5 Conclusions

In conclusion, the dam operation model has some limitations, as it produces negative flow, unrealistic relief flow and is too conservative with dam head levels. This results in not all ensemble members of the forecast having physical solution, and thus a number of possible solutions are lost. The S2S forecast runoff data has too short of a time period to use alone, as it produces unrealistic results that are not sensible in the long term. However, it is possible to use the historical runoff values from ERA5 reanalyses preceding the forecast date to extend the time range of runoff inputted to the model.

Though the calibration of the S2S runoff data was limited as it only used two summers of data, the calibrated extended S2S forecast has a flow solution that aligns well with upscaled ERA5 runoff data. The ensemble's 10-90 percentile range capturing the solution for high flow values, but not perform as well for low values after high values. Its ability to capture the solution for high flow values indicates potential in using the forecast, particularly ahead of extreme weather events. While the solutions aligned well with those upscaled ERA5 data, they followed a similar trend but did not have the same magnitudes as the solution from the ERA5 runoff data.

To improve the results from the forecast, more work has to be done to calibrate the upscaled ERA5 runoffs to the ERA5 runoffs. One possible way to achieve this could be by using more historical data to establish a more accurate relationship between the datasets. THe forecast could also be improved by downscaling S2S forecast to the $0.1^\circ \times 0.1^\circ$ grid, such that ERA5 data does not need to be upscaled for comparison.

Though results are not fully accurate to the ERA5 results, but the trends are very similar, and could allow dam management to use the forecast as guidance, or to scale the results from the forecast to get results closer to those from the ERA5 data. The most accurate forecasted results could be obtained by running the model with the extended S2S forecast when the newest forecast is released, thus allowing dam management to receive updated guidance on a frequent basis.

References

Christensen, K., and N. R. Maloney, 2005: *Self-Organised Criticality*, 325–330. Imperial College Press.

Enayati, M., O. Bozorg-Haddad, J. Bazrafshan, S. Hejabi, and X. Chu, 2020: Bias correction capabilities of quantile mapping methods for rainfall and temperature variables. *Journal of Water and Climate Change*, **12 (2)**, 401–419, doi:10.2166/wcc.2020.261, URL https://doi.org/10.2166/wcc.2020.261, https://iwaponline.com/jwcc/article-pdf/12/2/401/865958/jwc0120401.pdf.

Hirsch, P. E., S. Schillinger, H. Weigt, and P. Burkhardt-Holm, 2014: A hydro-economic model for water level fluctuations: Combining limnology with economics for sustainable development of hydropower. *PLOS ONE*, **9 (12)**, 1–26, doi:10.1371/journal.pone.0114889, URL https://doi.org/10.1371/journal.pone.0114889.

McGillivray, M. F., 2019: Complexity and networks, logbin function. Imperial College London.

Society, A. M., 2012: American Meteorological Society, URL https://glossary.ametsoc.org/wiki/Mesoscale_convective_system.